The wind-forced response on a buoyant coastal current: Observations of the western Gulf of Maine plume

Derek A. Fong

MIT/WHOI Joint Program in Oceanography, Woods Hole, MA 02543 U.S.A.

W. Rockwell Geyer

Woods Hole Oceanographic Institution, Woods Hole, MA 02543 U.S.A.

Richard P. Signell

United States Geological Survey, Woods Hole, MA 02543 U.S.A.

Journal of Marine Systems
submitted 1995 July 22
revised 1996 February 27

W.H.O.I. Contribution No. ????

Abstract

The freshwater plume in the western Gulf of Maine is being studied as part of an interdisciplinary investigation of the physical transport of a toxic alga. A field program was conducted in the springs of 1993 and 1994 to map the spatial and temporal patterns of salinity, currents, and algal toxicity. The observations suggest that the plume's cross-shore structure varies markedly as a function of fluctuations in alongshore wind forcing. Consistent with Ekman drift dynamics, upwelling favorable winds spread the plume offshore, at times widening it to over 50 km in offshore extent, while downwelling favorable winds narrow the plume width to as little as 10 km.

Using a simple slab model, we find qualitative agreement between the observed variations of plume width and those predicted by Ekman theory for short time scales of integration. Near surface current meters show significant correlations between cross-shore currents and alongshore wind stress, consistent with Ekman theory. Estimates of the terms in the alongshore momentum equation calculated from moored current meter arrays also indicate a dominant Ekman balance within the plume. A significant correlation between alongshore currents and winds suggests that interfacial drag may be important, although inclusion of a Raleigh drag term does not significantly improve the alongshore momentum balance.

1 Introduction

Freshwater runoff from rivers into the ocean has an important influence on the dynamics of many coastal regions. Since the river outflow tends to be less saline than the ambient coastal water, a surface plume typically forms as the buoyant riverine water spreads away from the river mouth. In the northern hemisphere, the Coriolis force turns the plume toward the right and traps the buoyant water against the coast, often forming a buoyancy-driven coastal current flowing in the direction of Kelvin wave propagation (e.g., Chao and Boicourt, 1986). However, winds may alter the structure of the plume due to upwelling and downwelling phenomena (e.g., Chao, 1988; Münchow and Garvine, 1993). This paper discusses a river plume in the Gulf of Maine, U.S.A. that shows significant influence from variations in wind forcing.

The Gulf of Maine is a region of continental shelf on the east coast of North America defined in extent by the Bay of Fundy to the north and Cape Cod to the south (Figure 1). The western Gulf of Maine plume (hereafter, GOM plume) is the result of river runoff from a series of rivers in the southwestern portion of the Gulf of Maine. The primary sources of the buoyant discharge for the Gulf of Maine are the Penobscot, Androscoggin/Kennebec, and Merrimack river systems (Figure 1). The majority of the freshwater inflow from the rivers occurs in the spring months with peak cumulative inflows of over 4000 m^3/s (J. Nielsen, United States Geological Survey, pers. commun., 1995).

A toxic dinoflagellate *Alexandrium tamarense* is found in the plume during the spring freshet (Hurst and Yentsch, 1981; Shumway et al., 1988); the toxin from this dinoflagellate is known to cause paralytic shellfish poisoning. Franks and Anderson (1992) proposed that the freshwater plume associated with these riverine discharges is directly responsible for the spatial and temporal distribution of *A. tamarense* blooms. Given the serious economic and health threats posed by this toxic alga, an interdisciplinary study was initiated to study transport properties of the GOM plume and its effect on the distribution of *A. tamarense*.

As is revealed in the data set presented below, the cross-shore extent of the GOM plume is strongly dependent on the direction and magnitude of wind forcing. This investigation examines the response and variability of the GOM plume's cross-shore structure and its relationship with the wind forcing.

In Section 2, we describe the field program. In Section 3, hydrographic and meteorological data are presented to illustrate the cross-shore variability of the GOM plume structure; a simple model is constructed to compare the observed hydrography with Ekman drift theory. In Section 4, moored current meter data are used to examine a shear alongshore momentum equation; discrepancies between Ekman theory and the observations are considered. The study's findings are discussed and summarized in Section 5.

2 Methods

During the spring months of 1993 and 1994, a total of 13 hydrographic surveys were conducted in the western Gulf of Maine. This study focuses primarily on data collected along a transect off Cape Porpoise (Figure 1). This particular transect was chosen for two reasons: (1) its location is coincident with moored current meter arrays, (2) it was the most frequently sampled transect in the field program. In April-July 1993, currents were measured at mooring B on the Cape Porpoise transect at the nominal depths of 5, 27, and 50 m with a Vector Measuring Current Meter (VMCM) and two Vector-Averaging Current Meters (VACM), respectively. For April-September 1994, currents were again measured at mooring B for the same depths, and an additional mooring A measured currents at nominal depths of 5 m and 27 m with a VMCM and VACM, respectively.

In addition, hourly wind speeds were recorded at a nearby meteorological buoy (Figure 1). These records were used to calculate cross- and alongshore components of wind stress using Large and Pond's (1981) quadratic drag law. The subsequent time series of wind stress and current meter measurements were low-pass filtered with a half power point at 33 hours (Beardsley et al, 1985). Combining the calculated wind stresses and hydrographic and moored data sets, we examine how the cross-shore plume structure varies as a function of local wind forcing.

3 Hydrographic surveys

Summary plots of alongshore wind stress, river inflow, and observed hydrography off of Cape Porpoise for 1993 and 1994 are shown in Figures 2 and 3, respectively. Plume widths based on salinity sections for each cruise are indicated using the 31 psu isohaline surface to define the extent of the plume. This choice is based on the observation that the 31 psu isohaline is almost always coincident with the maximum observed stratification. Based on a weighted average of winds prior to each hydrographic observation (using a one-sided Gaussian weighting with a decay time scale of three days), winds are classified as weak, upwelling favorable, or downwelling favorable, and denoted by a W, U, or D, respectively, in Figures 2 and 3. Weak winds are those with weighted averages less than 0.25 $dyne/cm^2$.

For both 1993 and 1994, the plume width is strongly influenced by the magnitude and direction of the alongshore wind forcing. Downwelling favorable (northeasterly) winds narrow the plume's cross-shore extent and confine it to a narrow region against the coast (Figure 4a). The minimum observed plume width was 10 km, during Cruise 2 in 1993 in strong downwelling winds. In contrast, upwelling favorable (southwesterly) winds tend to drive the plume waters more than 50 km offshore, often beyond the extent of our hydrographic surveys. Figure 4b provides an example of the influence of upwelling winds on the plume structure.

On the time scales of 1–2 weeks, the GOM hydrography suggests that the changes in observed plume width between the cruises are consistent with the direction of alongshore wind-forced response predicted by Ekman drift dynamics. This is similar to the behavior observed in previous modeling studies of wind-forced freshwater plumes (e.g., Chao, 1987; Csanady, 1977). In light of the apparent consistency between the GOM plume's cross-shore width and the alongshore winds with Ekman theory, we next consider a simple model.

If we approximate the plume as being a layer of light fluid of density ρ, and assume that the Ekman balance dominates the alongshore momentum equation, we can express the alongshore momentum balance by

$$fu = \frac{\tau^y}{\rho h}, \tag{1}$$

where h is the thickness of the plume, u depth-averaged cross-shore velocity within the plume, f is the Coriolis parameter, and τ^y is the alongshore wind stress.

Solving (1) for u and integrating in time, we can approximate an excursion length, L_e,

$$L_e = \int_{t_0}^{t_1} u dt = \int_{t_0}^{t_1} \frac{\tau^y}{\rho h f} dt. \tag{2}$$

Therefore, assuming the validity of (1) as the appropriate alongshore momentum balance, we can use (2) to calculate the width of the plume as a function of time given an initial plume width and time series of alongshore wind forcing.

Equation (2) was used to estimate the Ekman-induced changes in the offshore position of the plume and compare it with the observed changes between hydrographic surveys. The plume thickness for the calculations was estimated by linearly interpolating the observed plume thickness at the front. The thickness at the edge of the plume (rather than its average thickness) is the relevant h to use in (2) since the quantity of interest is the cross-shore motion of the plume boundary. The integration of (2) is also constrained such that the width of the plume never falls below a minimum value $L_c = 3\ km$, the baroclinic Rossby radius of the plume, which is roughly the lower limit of plume width based on modeling studies (e.g., Chao, 1988).

The results of the comparison between observed changes in plume width and equation (2) are shown in Table 1. There are large discrepancies for long integration time scales; however for the early cruises of 1994, the simple Ekman formulation predicts cross-shore plume excursions within 10 km of the observed motions when the time elapsed between cruises is less than 9 days. For example, equation (2) predicts the plume to widen by 41 km between cruises 5 and 6a, similar to the observed change of 33 km. In contrast, for the larger time integrations needed between cruises in 1993, prediction and observed motions often differ substantially. For Cruises 2 and 3 in 1993, equation (2) predicts the plume to widen 72 km while the observed plume width increases by only 10 km. Over these large time scales, the front loses its coherence. It appears that a new front formed before Cruise 3; the old front probably dissipated offshore, or has been transported downstream, out of the domain. Significant deviations also exist between predicted and observed plume widths in the latter cruises of 1994 despite short times of integration. These late observations are coincident with the low freshwater inflows, and hence, a weak plume. During these observations, the freshwater anomaly no longer dominates the density signal.

It is apparent from the hydrographic data that the fluctuations of the wind forcing, which typically occur on time scales of 1–2 days, severely decorrelates the observed plume between surveys. Given the typically large time intervals between the majority of cruises and the difficulty in applying this simple model to more than a few realizations, we next consider the time series data collected from the moored current meters at Cape Porpoise.

4 Moored Current Meter records

The moored current meters provide us with a means of evaluating the cross-shore motions of the plume temporally, in contrast to the hydrographic data which offer a detailed spatial picture of the plume's structure with coarse temporal resolution. The time series data of alongshore winds, cross-shore velocities, and salinities from the moorings in 1994 are shown in Figure 5. We will focus primarily on the 1994 data set below since it includes two moorings which provide some cross-shore spatial resolution.

As is visually apparent in Figure 5, the cross-shore velocities at the Cape Porpoise moorings also suggest a wind-forced plume behaving consistently with Ekman drift theory. Correlations between cross-shore near surface currents and alongshore wind stress are 0.53 for 1993 and 0.73 for 1994 (Table 2), both significant at the 99% confidence level (Glenberg, 1988). Complex correlations between wind stress and near-surface (5 m) velocity vectors reveal 59 and 66 degree clockwise veerings (of velocity with respect to the wind) for 1993 and 1994, respectively, further suggesting a dominant Ekman balance in the near surface waters. Also noteworthy are significant correlations between the cross-shore winds and alongshore currents, and the alongshore winds and alongshore currents (see Table 2). The former is indicative of Ekman dynamics playing an active role in the cross-shore momentum equation; we will address the second of the correlations later in the paper.

In order to better quantify the dominance of Ekman dynamics, we consider a layer-averaged alongshore momentum balance within the GOM plume:

$$\frac{\partial v_p}{\partial t} + u_p\frac{\partial v_p}{\partial x} + v_p\frac{\partial v_p}{\partial y} + fu_p = -\frac{\rho g}{\rho_0}\frac{\partial \eta}{\partial y} - \frac{gh}{2\rho_0}\frac{\partial \rho}{\partial y} + \frac{\tau^y}{\rho_0 h} - \frac{r\Delta v}{h}, \tag{3}$$

where u_p and v_p are the vertically-averaged cross- and along-plume currents, respectively, ρ is the plume density which is assumed to be independent of depth within the plume, $\frac{\partial\eta}{\partial y}$ is the alongshore surface slope, Δv is the difference in alongshore velocity between the plume and ambient waters at depth, and r is a Raleigh drag coefficient. Variations in sea surface elevations, η, are assumed to be much smaller than h. In waters beneath the plume, the vertically-averaged alongshore momentum balance can be expressed as:

$$\frac{\partial v_0}{\partial t} + u_0\frac{\partial v_0}{\partial x} + v_0\frac{\partial v_0}{\partial y} + fu_0 = -\frac{\rho g}{\rho_0}\frac{\partial \eta}{\partial y} - \frac{gh}{\rho_0}\frac{\partial \rho}{\partial y}, \tag{4}$$

where the stresses in the waters below the plume are assumed to be small. Subtracting (4) from (3) to eliminate the surface slope term yields a shear alongshore momentum equation:

Ekman balance

$$\frac{\partial \Delta v}{\partial t} + \Delta(u\frac{\partial v}{\partial x}) + \Delta(v\frac{\partial v}{\partial y}) + f\Delta u = \frac{gh}{2\rho_0}\frac{\partial \rho}{\partial y} + \frac{\tau^y}{\rho_0 h} - \frac{r\Delta v}{h}, \tag{5}$$

A B C D E F G

where $\Delta u = u_p - u_0$, $\Delta v = v_p - v_0$, and Δ preceding the nonlinear terms B and C denote differences of each term between the plume and ambient waters.

Terms A, B, D and F can be calculated from the two moorings deployed at Cape Porpoise in the spring of 1994. The acceleration and Coriolis force terms on the left-hand side of (5) are estimated by averaging the shear velocities (Δu and Δv) at moorings A and B. The nonlinear term B is estimated by computing the gradient of alongshore velocities measured between the moorings at the two depths and subtracting $u\frac{\partial v}{\partial x}|_{25m}$ from $u\frac{\partial v}{\partial x}|_{5m}$. The alongshore plume wind stress (term F) is computed using wind measurements from the meteorological buoy as discussed in Section 2, and linearly interpolating the plume thickness h at the hydrographic survey stations coincident with the mooring locations.

The resulting time series of terms A, B, D, and F are shown in Figure 6. The top panel compares the shear Coriolis force term with the surface wind stress term. The second plot contains the same two variables, but the contribution of the mean shear over the record of 7 cm/s has been removed to make it easier to compare the variations. The third and fourth panels are the cross-shore advection of alongshore momentum and time dependencies, respectively.

Ekman balance

Consistent with the hydrography and time series correlations, the surface wind stress and shear Coriolis force terms have the largest magnitudes and are highly correlated: 0.75 (see Table 3). The nonlinear term B is consistently small except for one short-lived event. The alongshore acceleration (term A) is of moderate size, but is not correlated with the wind stress.

Despite the high correlations between the wind stress and Coriolis terms, the time series (Figure 6) reveal several events in which there is a marked discrepancy between the two terms. These discrepancies are due in part to the crudeness of the layer-averaged approach, particularly during strong upwelling when the plume may be thinner than 5 m, the depth of the near-surface current meters. Some of the discrepancies are also due to other terms in the momentum balance.

Other contributors to the alongshore momentum balance

As has been discussed, $\frac{\partial \Delta v}{\partial t}$ and $\Delta(u\frac{\partial v}{\partial x})$ are significantly smaller than either the Coriolis or wind stress terms. Furthermore, neither of these terms are correlated with the wind stress (Table 3). If we account for these two terms in trying to balance out the wind stress (i.e, $\frac{\partial \Delta v}{\partial t} + \Delta(u\frac{\partial v}{\partial x}) + f\Delta u$ vs. $\frac{\tau^y}{\rho h}$), we get a lower correlation (0.66). Figure 7a shows the comparison of the wind stress to the other terms.

There are three terms in (5) which we could not compute from our time series data: the alongshore advection of alongshore momentum, the baroclinic pressure gradient, and the interfacial drag. In order for the first two of these terms to be important, the alongshore length scales of variability must be small, i.e., less than 10 km. The hydrographic data only resolved scales of 30 km in the along-shore direction, over which there was minimal variability during downwelling conditions and modest variations during upwelling. It is possible that there were unresolved variations at smaller scales, but there is no evidence for it.

It is also difficult to specify the friction term G. If we perform an analysis similar to Lentz's (1995) analysis of friction in the Amazon River plume we can obtain an estimate of r. Using an empirical fit for the observed variations in wind stress, along-plume, and across-plume velocities at the moorings for both 1993 and 1994, we estimate a Rayleigh drag coefficient $O(10^{-4})\ m/s$. This value is surprisingly large. Interpreting r as the product of a mean velocity times a drag coefficient (i.e., $r = C_i|\Delta\vec{u}|$ where $\Delta\vec{u} \sim (1\times10^{-1}\ m/s)$ is the difference in velocity between the two layers), we estimate $C_i \sim O(10^{-3})$, almost an order of magnitude larger than Lentz (1995) found in the Amazon River plume, and comparable to a bottom drag coefficient.

Using the above estimate of r, the correlation between $(f\Delta u + \frac{rv_p}{h})$ and $\frac{\tau^y}{\rho h}$ is 0.83. Figure 7b plots the sum of $(\frac{\partial \Delta v}{\partial t} + \Delta(u\frac{\partial v}{\partial x}) + f\Delta u + \frac{rv_p}{h})$ vs. $\frac{\tau^y}{\rho h}$. The inclusion of the interfacial friction term is not a significant improvement from the previous balance neglecting it, and does not consistently account for the difference between the wind stress and Coriolis terms in Figure 6. Thus, this analysis does not provide conclusive evidence of a large interfacial drag term; only that such a magnitude would be consistent with the data. It is plausible that the correlation between the alongshore velocity and alongshore winds are purely an Ekman-based response generated by a coupling of the two momentum equations: the alongshore wind is responsible for a cross-shore Ekman transport that displaces the isohalines, thereby readjusting geostrophic velocities in the cross-shore momentum balance, and resulting in a correlation between along-shelf winds and along-shelf currents without appreciable interfacial drag.

5 Discussion and Summary

The western Gulf of Maine plume's responses to different orientations of wind forcing have tendencies consistent with Ekman drift dynamics. Using a simple, idealized model of Ekman dynamics, we find qualitative agreement with the observed plume's cross-shore motions and that predicted by the model; however, the applicability of the model is limited to short periods of integration over which the plume front maintains its coherence. The wind fluctuations over time scales of a few days suggest that the correlation time scales of the plume are short.

The moored observations also support the dominance of Ekman dynamics: cross-shore plume velocities are highly correlated with alongshore winds and tend to dominate the shear alongshore momentum balance. Alongshore acceleration effects are non-trivial although they do not improve the balance of terms in the momentum equation. This suggests that some other terms such as friction and the along-coast baroclinic pressure gradient may be important. An empirical analysis of the interfacial friction suggests a large Rayleigh friction factor, although it may be an artifact of the coupling between the two momentum equations.

Some of the discrepancies between the observed time series of wind stress and Coriolis terms are likely the result of errors in accurately specifying the plume thickness as a function of time. The plume's thickness is a quantity which is likely to vary over short-time scales. The plume's thickness is related to both the orientation and magnitude of wind forcing. For downwelling favorable winds, the plume is typically thick, sometimes nearing 20 m thickness. In contrast, thinner plumes are predominantly found under upwelling favorable wind conditions. There may be a correlation between the wind stress and plume thickness, which would lead to an asymmetric response to variations in wind forcing.

The moored current meters exhibit a significant mean offshore surface velocity (over 5 cm/s) that is not explainable by any mean wind-forcing conditions. There is little suggestion that this is a result in measurement error, nor is there any indication from the data that there is some underlying physical process that would produce a mean offshore surface current. A significant along-coast density gradient would be required to support a 5 cm/s mean flow; this does not seem plausible based on these observations nor studies of the Gulf of Maine (e.g., Brown and Irish, 1992). The offshore mean in the surface flow field may be the result of some asymmetry in the plume's response to upwelling and downwelling winds causing a rectification of the Ekman transport offshore. Alternatively, there could be small scale bathymetric variations that are not resolved by the available bathymetric data, which cause a local deflection of the the alongshore currents at Cape Porpoise.

One of the severe limitations of the above analysis is the approximation of the GOM plume as a two-dimensional phenomenon. The hydrographic observations suggest this assumption is primarily valid during downwelling favorable wind conditions; for strong upwelling favorable wind conditions, there is much greater alongshore variability. Downstream of Cape Porpoise, in the southern portions of the western Gulf of Maine, the cross-shore topography diverges (see Figure 1), leading to likely variability in alongshore plume behavior. In addition, the variation in freshwater discharge is an inherent problem in considering the plume over the long time scales between hydrographic surveys. The water mass observed during one hydrographic survey is clearly different than waters observed in a subsequent one.

We have also neglected to consider the coupling of the cross-shore momentum equation and how cross-shore winds might drive cross-shore plume motions. Despite the smaller magnitude of the cross-shore wind component with respect to the alongshore component, a small, yet significant (to 95% confidence level) correlation between alongshore and cross-shore winds in 1993 suggests that the cross-shore winds may play a role in determining cross-shore plume variability.

The inherent simplifications of using the moored near-surface measurements of velocity to describe a depth-averaged plume motion is another source of error; the approximation of the plume as a layer of homogeneous light water overlying fixed density coastal waters is a crude picture of a plume. The detailed vertical and horizontal structure of the plume are obviously important for a number of processes including the alongshore transport within the plume and the influence of wind forcing with respect to depth.

Issues related to the alongshore transport in the GOM plume are currently being studied. A suite of three-dimensional numerical modeling experiments are being conducted which address some of the limitations of this study. A combination of such modeling studies with additional studies of the moored current meter and surface drifter data sets should further our understanding of the western Gulf of Maine plume's dynamics.

Acknowledgments. We are pleased to acknowledge the helpful comments of R. Garvine, G. Gawarkiewicz, and S. Lentz. The comments and suggestions from two anonymous reviewers also helped improve the paper. We would also like to thank J. Nielsen and the USGS for generously supplying the river runoff data. Special thanks to B. Keafer for his dedication and perseverance in collecting the hydrographic data presented. DAF was supported by a National Science Foundation Graduate Fellowship. WRG, RPS, and the field observations were funded by the Gulf of Maine Regional Marine Research Program grant UM-S227.

References

Beardsley, R.C., Limeburner, R. and Rosenfield, L., 1985. CODE-2 Moored Array and Large-Scale Data Report. Woods Hole Oceanographic Institution, WHOI 85-35, 234 pp.

Brooks, D.A., 1994. A model study of buoyancy-driven circulation in the Gulf of Maine. Journal of Physical Oceanography, 24: 2387-2412.

Brown, W.S. and Irish, J.D., 1992. The annual evolution of geostrophic flow in the Gulf of Maine: 1986-1987. Journal of Physical Oceanography, 22: 445-473.

Chao, S.-Y., 1988. Wind-driven motion of estuarine plumes. Journal of Physical Oceanography, 18: 1144-1166.

Chao, S.-Y. and Boicourt, W.C., 1986. Onset of estuarine plumes. Journal of Physical Oceanography, 16: 2137-2149.

Csanandy, G.T., 1977. Intermittent full upwelling in Lake Ontario. Journal Geophyscial Research, 82: 397-419.

Franks, P.J.S. and Anderson, D.M., 1992. Alongshore transport of a toxic phytoplankton bloom in a buoyancy current: Alexandrium tamarense in the Gulf of Maine. Marine Biology, 112: 153-164.

Glenberg, A.M., 1988. Learning from data: an introduction to statistical reasoning, Harcourt Brace Jovanovich, Publishers, 535 pp.

Hurst, J.W. and Yentsch, C.M., 1981. Patterns of intoxication of shellfish in the Gulf of Maine coastal waters. Canadian Journal of Fish and Aquatic Sciences, 38: 152-156.

Large, W.G. and Pond, S., 1981. Open ocean momentum flux measurements in moderate to strong winds. Journal of Physical Oceanography, 11: 324-336.

Lentz, S.J., 1995. The Amazons River Plume during AMASSEDS: Subtidal current variability and the importance of wind forcing. Journal of Geophysical Research, 100: 2377-2390.

Münchow, A. and Garvine, R.W., 1993. Buoyancy and wind forcing of a coastal current. Journal of Marine Research, 51: 293-322.

Shumway, S., Sherman-Caswell, S. and Hurst, J.W., 1988. Paralytic shellfish poisoning in Maine: monitoring a monster. Journal of Shellfish Research, 7: 643-52.

Figure Captions

Figure 1. The study region: the western Gulf of Maine. The two major sources of freshwater are the Kennebec/Androscoggin and Merrimack River systems. The dashed line indicates CTD stations along the Cape Porpoise transect. The locations of moored current meter arrays A and B and the meteorological buoy are also indicated. The Penobscot river, not shown, is located to the north-east of the plotted region.

Figure 2. 1993 observations in the western Gulf of Maine. Time series of winds measured at the meteorological buoy and freshwater inflow from the Penobscot, Kennebec/Androscoggin, and Merrimack river systems are shown. The timing of hydrographic surveys at the Cape Porpoise transect are indicated by the gray vertical bands. The observed plume width during the surveys are indicated in km with a classification of the winds preceding each survey; D indicates downwelling favorable winds prior to the survey while upwelling favorable winds are labeled with a U; weak winds are denoted by a W.

Figure 3. 1994 observations in the western Gulf of Maine (as in Figure 2).

Figure 4. Horizontal sections of salinity at 2.5 meters depth based on Hydrographic surveys (stations indicated by dots). (a) Downwelling favorable wind conditions (Cruise 93-3: April 28-30, 1993), (b) Upwelling favorable conditions (Cruise 94-6a: June 1-3, 1994).

Figure 5. Time series of alongshore wind stress, salinity and cross-shore velocities measured at Cape Porpoise in 1994.

Figure 6. Time series of different terms in the shear alongshore momentum equation. Subscripts indicate partial differentiation.

Figure 7. Balancing the shear alongshore momentum: (a) excluding interfacial friction (b) including interfacial friction.

Table 1. Observed change in plume width off of Cape Porpoise vs. Prediction from Equation (2) for 1993 and 1994.

Year	Starting Cruise	Ending Cruise	Integration time (days)	Intial Width (km)	Observed Change (km)	Predicted Change (km)
1993	2	3	15.5	10	10	72
1993	3	5	26.5	21	-5	35
1993	5	6	10.5	16	>11	18
1994	2a	2b	3.6	19	11	5
1994	2b	3	6.9	30	<-8	-12
1994	4	5	4.0	16	1	6
1994	5	6a	8.2	17	33	41
1994	6a	6b	2.8	50	-27	2
1994	6b	7	6.1	23	2	22
1994	7	9	20.0	25	>25	113

Table 2. Low-Passed Correlation Coefficients for April 15-June 15 for 1993 and 1994 (top and bottom coefficients in table entries, respectively).

	year	Alongshore Wind Stress	Cross-shore Wind Stress	Alongshore Velocity	Cross-shore Velocity
Alongshore Wind Stress	1993	1	-0.37	0.51	0.53
	1994	1	-0.18	0.43	0.73
Cross-shore Wind Stress	1993		1	-0.39	-0.08
	1994		1	-0.47	0.02
Alongshore Velocity	1993			1	-0.06
	1994			1	0.11
Cross-shore Velocity	1993				1
	1994				1

Zero-lag correlation coefficients were very near maximum lagged correlations. For a 50-hour integral time scale, correlations of 0.38, and 0.49 are significant at the 95% and 99% levels, respectively. (Glenberg, 1988)

Table 3. Low-Passed Correlation Coefficients for April 30-June 10, 1994 for shear alongshore momentum components.

	$\frac{\tau^y}{\rho h}$	$f\Delta u$	$\Delta(u\frac{\partial v}{\partial x})$	$\frac{\partial \Delta v}{\partial t}$	$\frac{r\Delta v}{h}$
$\frac{\tau^y}{\rho h}$	1	**0.75**	-0.15	0.11	**0.64**
$f\Delta u$		1	0.23	0.03	0.32
$\Delta(u\frac{\partial v}{\partial x})$			1	0.09	0.06
$\frac{\partial \Delta v}{\partial t}$				1	0.01
$\frac{r\Delta v}{h}$					1

For a 55-hour integral time scale, bold-faced entries indicate correlations significant at the 99% level (Glenberg, 1988).

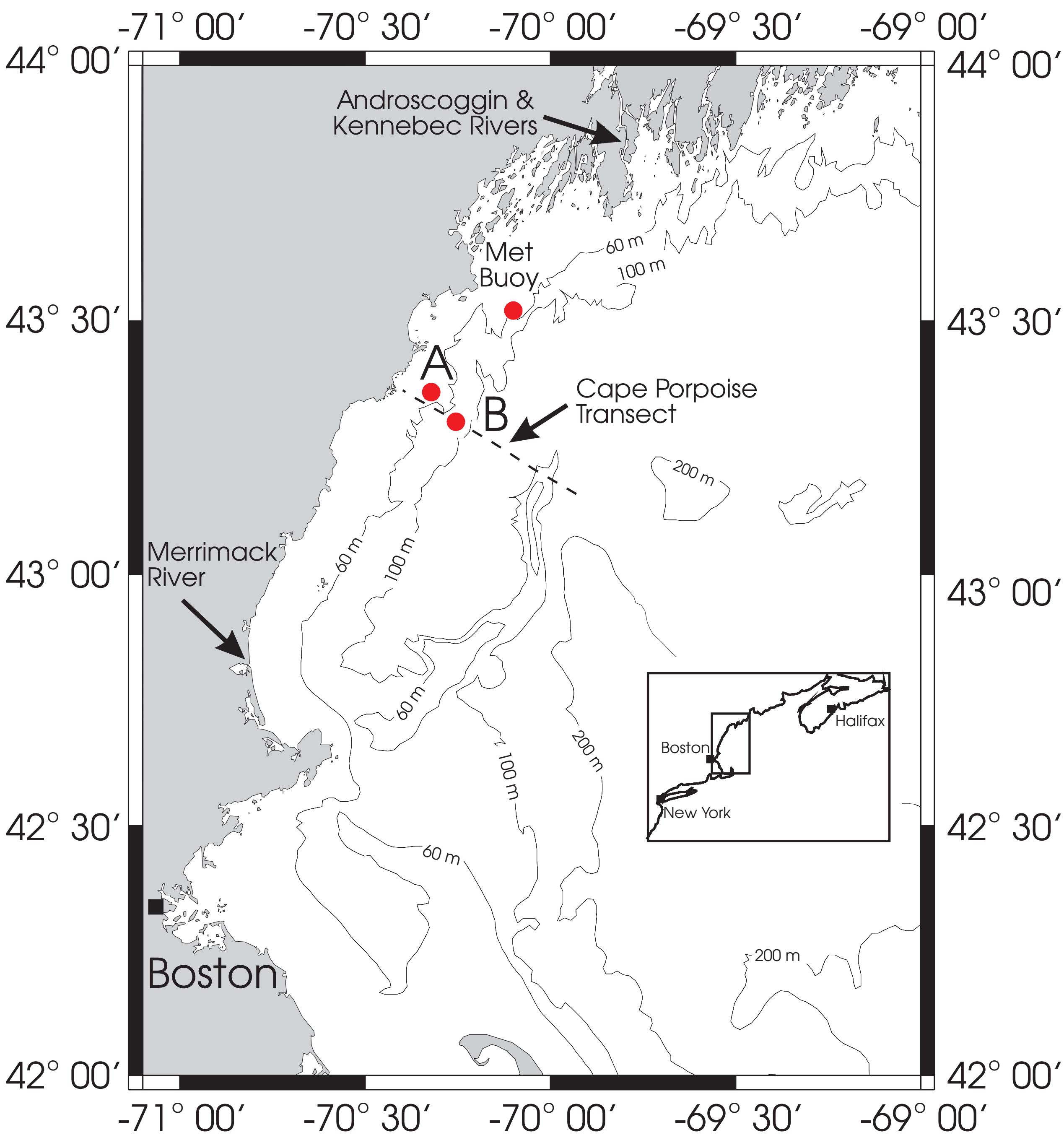
-71° 00′
-70° 30′
-70° 00′
-69° 30′
-69° 00′
44° 00′
43° 30′
43° 00′
42° 30′
42° 00′
Androscoggin &
Kennebec Rivers
Met
Buoy
60 m
100 m
A
B
Cape Porpoise
Transect
200 m
Merrimack
River
60 m
100 m
60 m
100 m
200 m
60 m
200 m
Boston
Halifax
Boston
New York

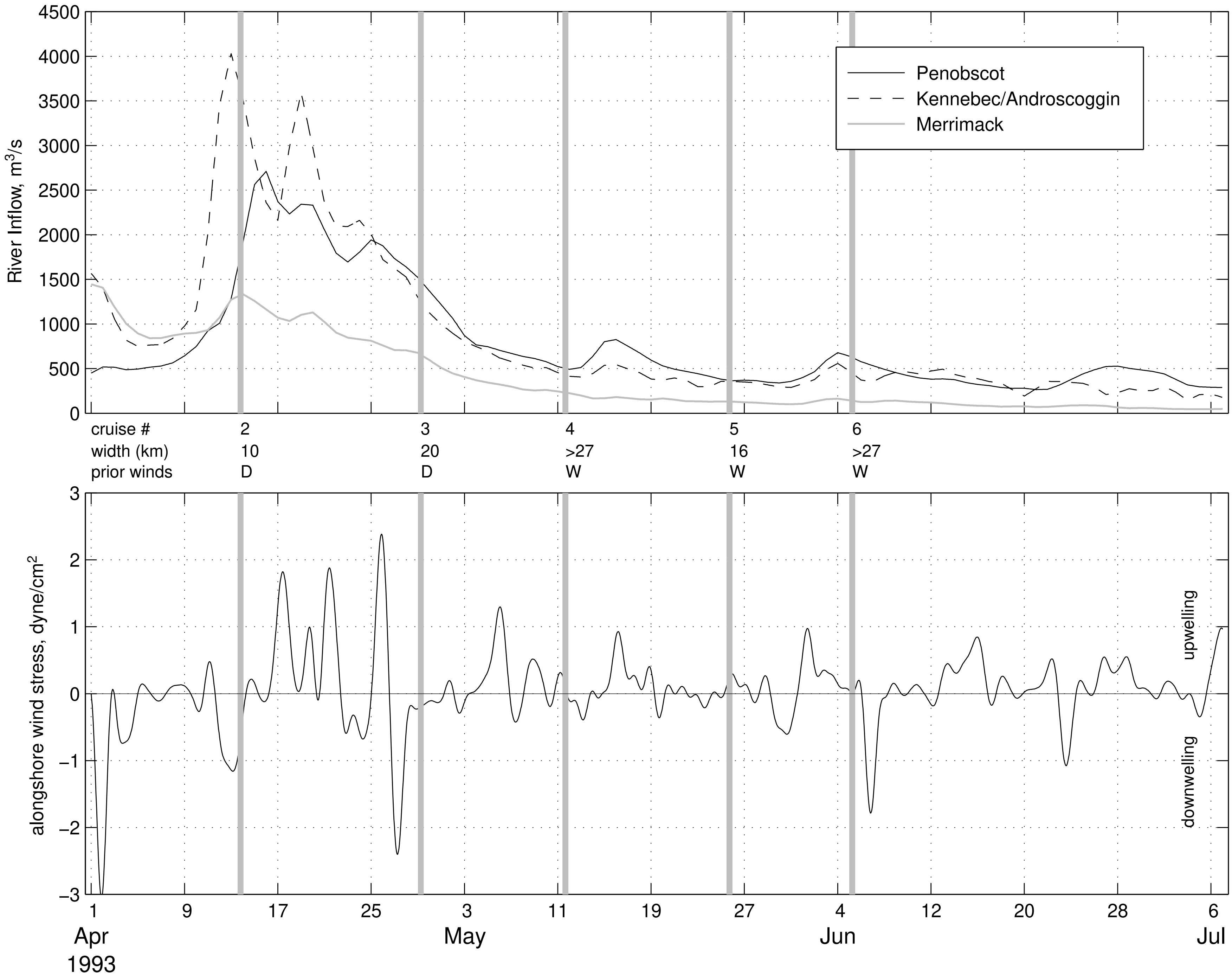
Penobscot
Kennebec/Androscoggin
Merrimack
River Inflow, m^3/s
4500
4000
3500
3000
2500
2000
1500
1000
500
0
cruise # 2 3 4 5 6
width (km) 10 20 >27 16 >27
prior winds D D W W W
alongshore wind stress, dyne/cm^2
3
2
1
0
−1
−2
−3
upwelling
downwelling
1 9 17 25 3 11 19 27 4 12 20 28 6
Apr
1993
May
Jun
Jul

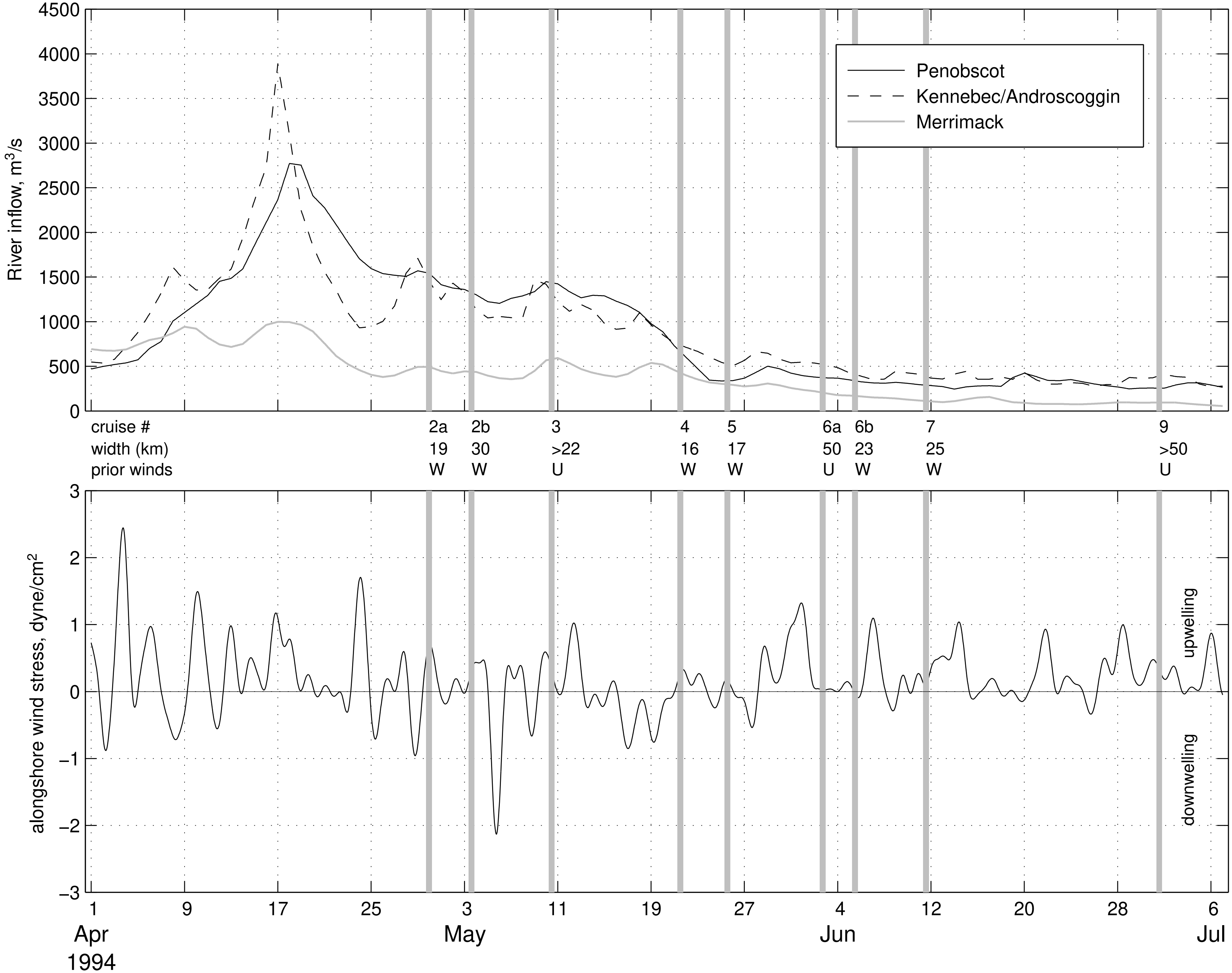
Penobscot
Kennebec/Androscoggin
Merrimack
River inflow, m^3/s
cruise #
width (km)
prior winds
2a 19 W
2b 30 W
3 >22 U
4 16 W
5 17 W
6a 50 U
6b 23 W
7 25 W
9 >50 U
alongshore wind stress, dyne/cm^2
upwelling
downwelling
Apr 1994
May
Jun
Jul

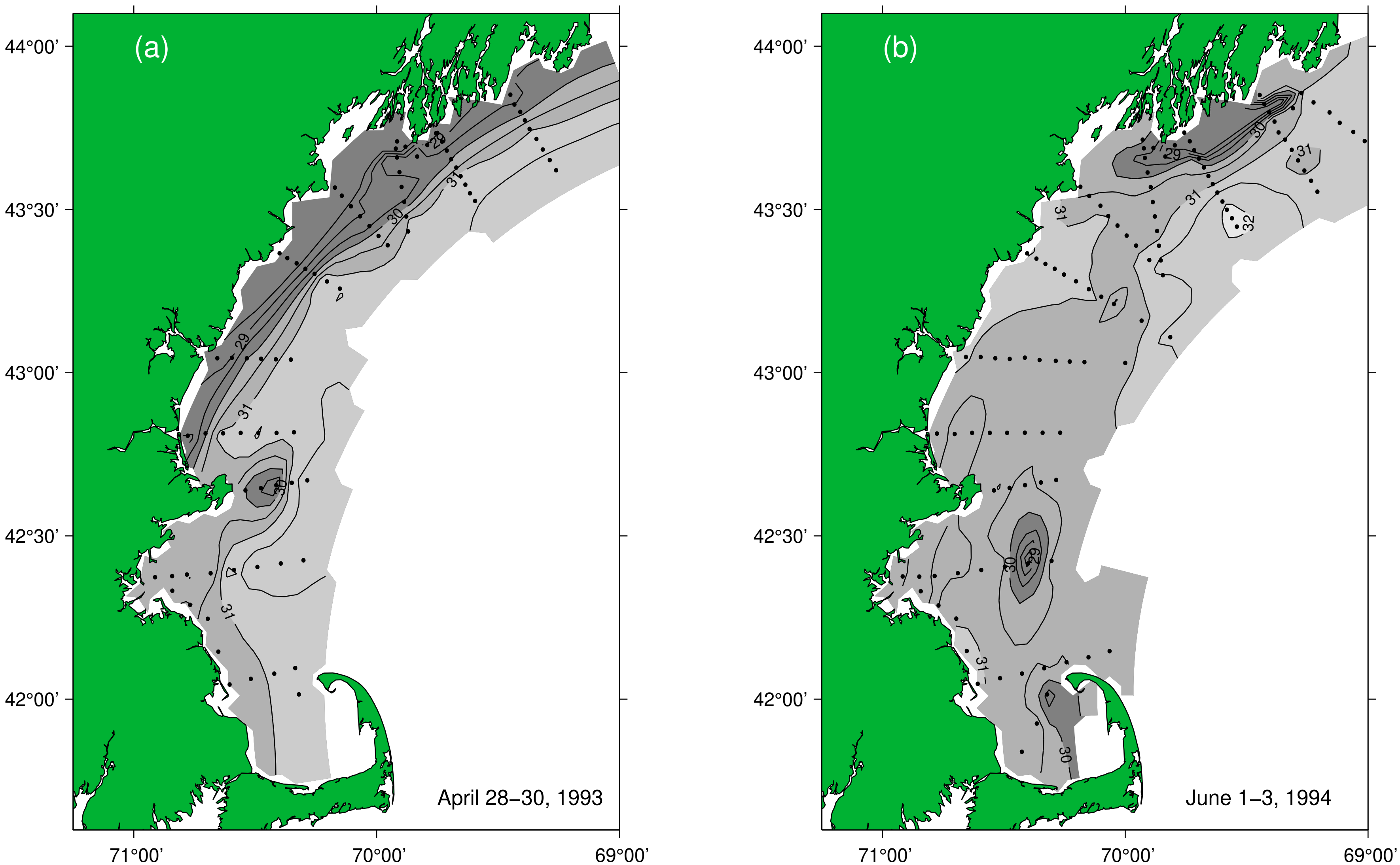
(a)
April 28–30, 1993
(b)
June 1–3, 1994
44°00'
43°30'
43°00'
42°30'
42°00'
71°00'
70°00'
69°00'
29
30
31
32

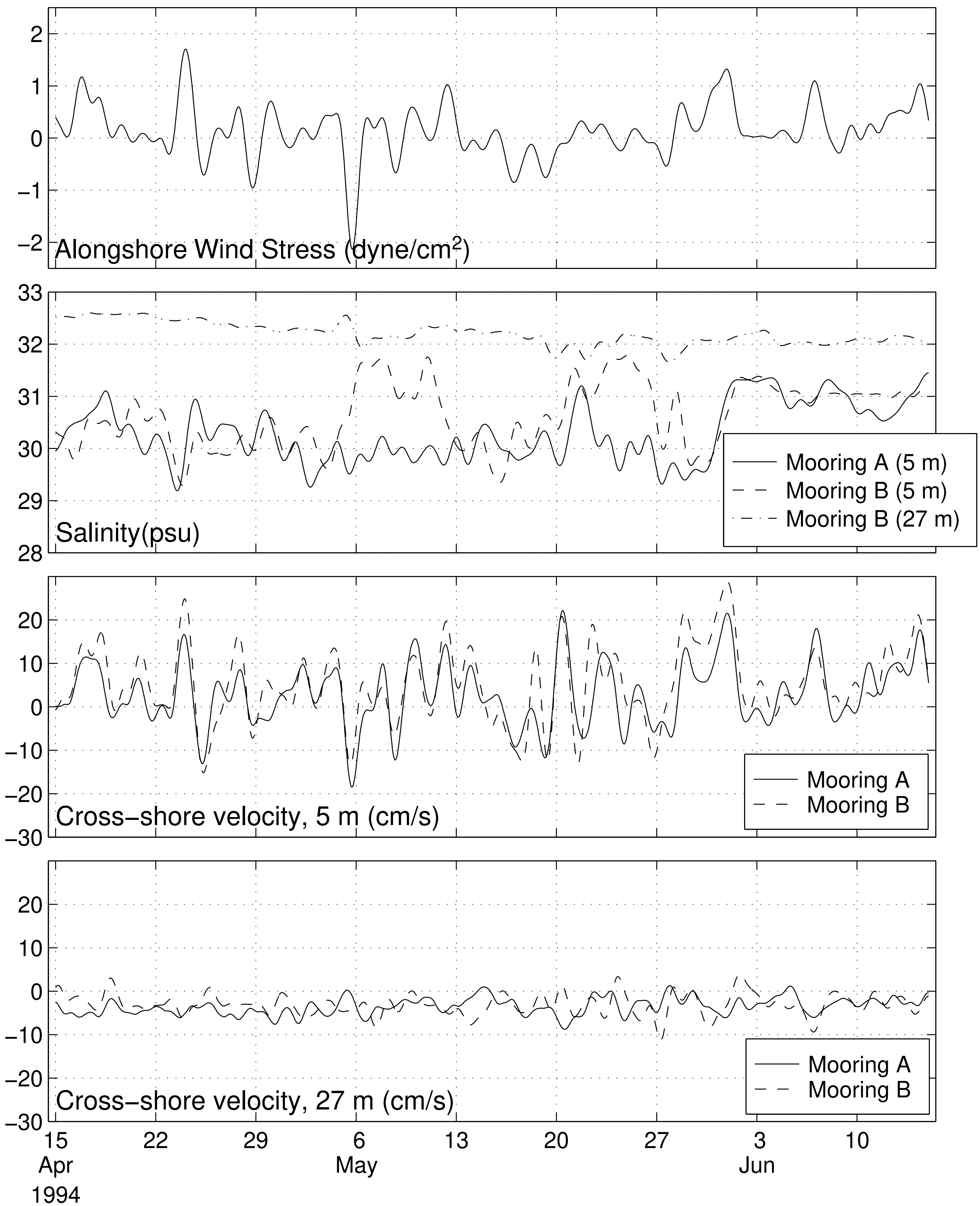

Alongshore Wind Stress (dyne/cm²)
2
1
0
–1
–2
Salinity(psu)
33
32
31
30
29
28
Mooring A (5 m)
Mooring B (5 m)
Mooring B (27 m)
Cross–shore velocity, 5 m (cm/s)
20
10
0
–10
–20
–30
Mooring A
Mooring B
Cross–shore velocity, 27 m (cm/s)
20
10
0
–10
–20
–30
Mooring A
Mooring B
15
22
29
6
13
20
27
3
10
Apr
May
Jun
1994

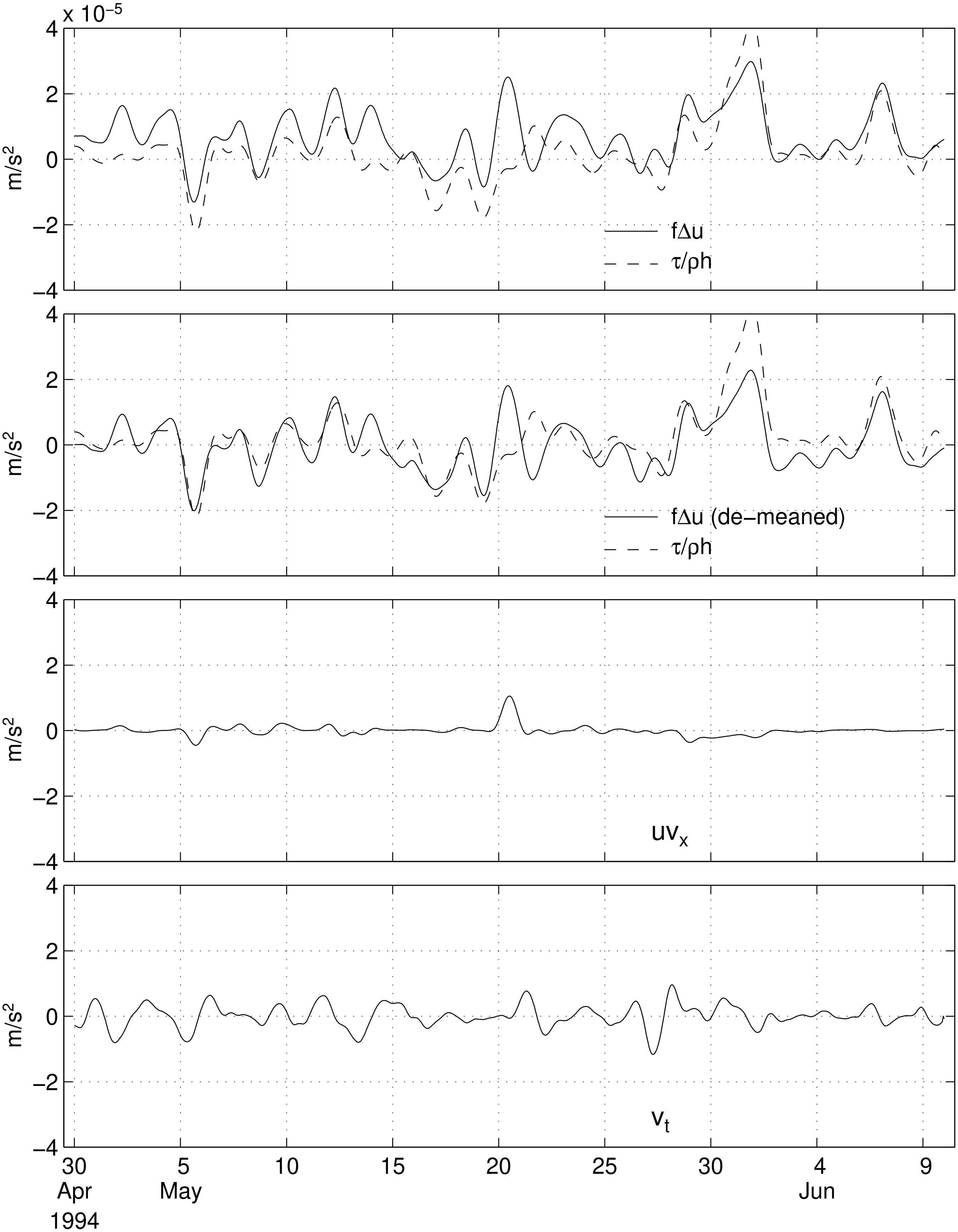

x 10^−5
m/s²
fΔu
τ/ρh
fΔu (de−meaned)
τ/ρh
uv_x
v_t
30
Apr
1994
5
May
10
15
20
25
30
4
Jun
9

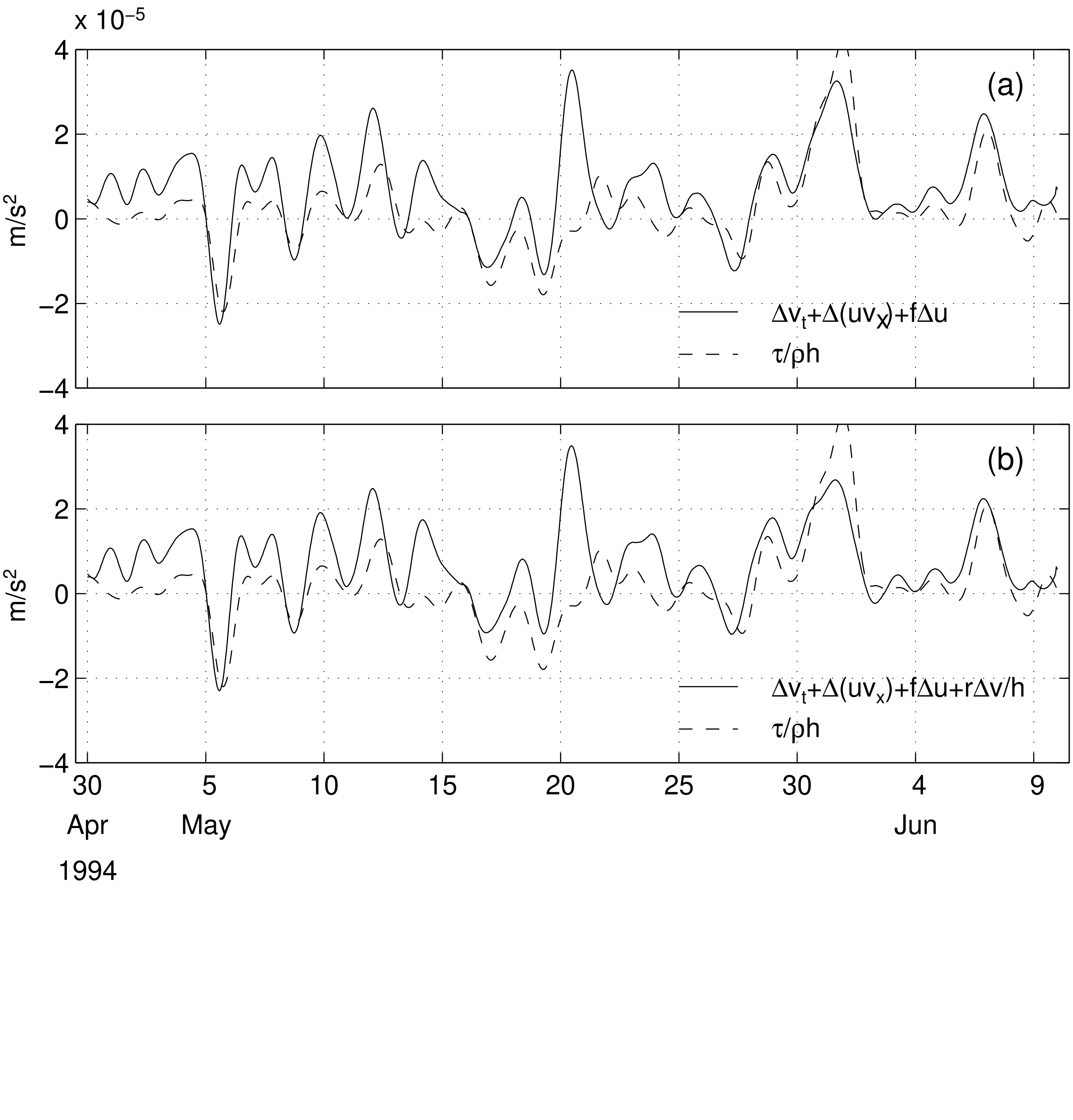

x 10^−5
(a)
Δv_t+Δ(uv_x)+fΔu
τ/ρh
(b)
Δv_t+Δ(uv_x)+fΔu+rΔv/h
τ/ρh
m/s^2
m/s^2
4
2
0
−2
−4
30
5
10
15
20
25
30
4
9
Apr
May
Jun
1994